



Influence of Giant Reed Fibers on Mechanical, Thermal, and Disintegration Behavior of Rotomolded PLA and PE Composites

Luis Suárez¹ · Zaida Ortega² · Francisco Romero¹ · Rubén Paz¹ · María D. Marrero¹

Accepted: 28 July 2022
© The Author(s) 2022

Abstract

This paper assesses the modifications in the properties of rotomolded polyethylene (PE) and polylactic acid (PLA) composites obtained with 5 and 10% giant reed fibers, mainly focusing on the alterations due to a bio-disintegration process. Thermal properties (melting temperature and crystallinity degree), morphology (via optical and scanning electron microscopy), and chemical changes (by Fourier Transformed Infrared spectroscopy) were studied. Composites with untreated and NaOH-treated fibers were obtained, finding that this treatment does not improve the mechanical performance of composites due to increased porosity. The introduction of natural fibers into a PE matrix does not significantly modify the thermal and bio-disintegration properties of the rotomolded material. Regarding mechanical properties, PE-composites show increased tensile modulus and reduced impact and tensile strength than the matrix. On the other hand, PLA composites show lower impact and flexural strength than neat PLA, remaining the rest of the mechanical properties unchanged regardless of the fibers' addition. The incorporation of *Arundo* fibers modifies to a great extent the thermal and degradation behavior of the PLA matrix.

Keywords Rotational molding · Characterization · Bio-disintegration · PLA · PE · Giant reed

Introduction

Rotational molding is a well-established technology that produces hollow parts with good surface quality and mechanical properties. The range of available materials is not as comprehensive as for other polymer processing technologies. For this reason, several authors have focused on using materials adapted to rotomolding specificities. Polyethylene (PE) accounts for more than 90% of the rotomolding market [1], while polylactic acid (PLA) is the second most used one [2–6] due to its recyclability, biodegradability, and good properties. Some studies with other materials, such as PE/PLA blends [6], polycaprolactone (PCL) [7], or recycled materials, can be found in the literature. For recycled materials, the use of up to 35% of cable waste in a PE matrix has been proposed [8]. The parts made with fully recycled plastic residues have also been studied, showing low mechanical

properties due to the difficulty of obtaining PE pure fractions from post-consumer plastics [9]. Copper slag has been introduced into a PLA matrix up to 20%, bringing a composite material stiffer and harder than the polymer itself [10]. Finally, some attempts to recycle PLA fractions have been performed [11, 12], paying particular attention to the degradation that may arise in the polymer due to reprocessing.

On the other hand, the literature shows limited rotomolding studies using fillers or reinforcements from natural fibers or waste materials. Regarding natural fibers, Torres and Aragon found that the introduction of up to 10% in weight (w/w) of cabuya and sisal fiber noticeably reduced the impact properties of the composite without any improvement in tensile properties [13], while Wang et al. reported no modification of these properties for 10% w/w flax composites [14]. Ortega et al. produced composites with 5% w/w of banana and abaca fibers with significant improvements in mechanical properties, except for impact strength [15]. Cisneros-López et al. have also found no statistical differences in mechanical properties for composites containing up to 10% w/w of agave fibers in a PLA matrix, while higher loadings of fibers result in an important decrease in mechanical performance [16]. Hejna et al. obtained composites with up to 20% w/w of wheat bran, although only those with up

✉ Zaida Ortega
zaida.ortega@ulpgc.es

¹ Departamento de Ingeniería Mecánica, Universidad de Las Palmas de Gran Canaria, 35017 Las Palmas, Spain

² Departamento de Ingeniería de Procesos, Universidad de Las Palmas de Gran Canaria, 35017 Las Palmas, Spain

to 5% content did not show significant loss of mechanical properties [1]. Buckwheat husks have been used up to 30% w/w for composites production, although with substantial reductions in mechanical properties [17]. The use of compatibilizers, such as maleated PLA or glycidyl methacrylate grafted PLA, increases the amount of fiber used up to 20% (w/w) [18, 19]. However, this implies a further step of processing and, thus, higher cost. 10% loading (in weight) is commonly used for rotational molding [20].

Some authors have pointed out that the voids found in rotomolded parts are responsible for the reduction in mechanical properties of composites [16]. The lack of continuity in the matrix hinders the formation of the crystals. The deficient contact between the fiber and the matrix avoids a good stress transfer between both components. Particle size distribution has also been proven to significantly affect the properties of rotomolded parts [18–20] and the amount of filler introduced into a PE or PLA matrix [17, 21].

This paper focuses on using fibers obtained from *Arundo donax* L. stems as fillers of rotationally molded PE or PLA matrixes. This species, also known as common reed or giant reed, is a rhizomatous grass with a quick growth rate, which makes it especially interesting due to the high amount of biomass available. Different high-added value products can be obtained from this plant in a biorefineries context: fibers [22–24], bioethanol [25, 26], xylose [27], levulinic acid [28, 29] or bio-polymers [30, 31]. Different works in literature propose its use as raw material for oil spill recovery [32], soil remediation [33], or paper obtaining [34]. Rajkumar and collaborators have proposed using PET as the matrix of composites with peeled stems [35]. Similarly, several authors have used the shredded plant to produce panels using natural binders, such as citric acid, with applications in acoustic and thermal insulation [36, 37].

Some authors have proposed obtaining fibers from reed and using them for composites, especially by compression molding. For example, Fiore et al. have obtained reed-PLA composites with higher modulus than the matrix [38], while Suárez et al. proposed using these fibers in PE and PP matrixes [24] with significant increases in elastic modulus. Monsalve Alarcón and collaborators [39] obtained composites with a PU-natural resin with improved stiffness. Other authors have explored *Arundo*'s use as epoxy fillers reinforcement [40, 41], providing higher tensile moduli and lower strength. Finally, Ortega et al. have produced rotationally molded PE-composites with this filler, with a drop in mechanical properties [21].

On the other hand, the impact of polymers on the environment is undeniable due to their abuse and long lifecycle. In recent years, biodegradable plastics' presence in consumer products, mainly in packaging, has been widely increased to overcome this problem. It is essential to differentiate between bio-degradation and bio-disintegration,

as these terms are often confused. Degradation refers to the modification of macromolecules due to their release from the primary chemical chain, and it is often associated with a decrease in performance. However, it is usually preferred to refer to it as the decrease in molecular weight. The term biodegradation refers to the degradation process performed by living cells and not by enzymes isolated from them. So, the degradation tests usually performed in literature, especially in the bio-materials field, which assess the modifications of a material due to enzyme action, cannot be considered biodegradation assays. Finally, disintegration relates to the breakage of a sample into smaller parts than the original size [42].

Plastics biodegradation is greatly affected by the nature of the material (chemical structure and functional groups, crystallinity, molecular weight, additives), the type of organism involved in the process (bacteria, fungi, algae), and the conditions (temperature, humidity, pH) in which the process takes place [43]. PLA has often been classified as a biodegradable material, although this process only takes place under a compost environment, that is, in the presence of appropriate microorganisms and elevated temperature [44]. For these authors, the main factors affecting the PLA biodegradation process are polymer molecular weight (the higher the weight, the slower the degradation) and the L/D monomer ratio (higher crystallinity leads to lower degradation). Abiotic degradation can take place if the material is immersed in hot water and is considered crucial for biodegradation of PLA, as it leads to ester links hydrolysis [44, 45].

Most literature about PLA biodegradation focuses on processes performed at thermophilic conditions (around 58 °C) [46–48]. However, some authors suggest using mesophilic conditions (37 °C) [49], as most municipal waste treatment plants operate in these conditions and also because these are usually more stable and have lower energy requirements.

This paper deals with the assessment of the properties of composite parts obtained by rotational molding, using two different matrixes: PE and PLA and giant reed (*Arundo donax*) fibers at 5 and 10 wt % loading. Mechanical behavior, morphology, and bio-disintegration of composite materials have been assessed. Bio-disintegration assays have been performed following the procedure in UNE-EN 20200:2015, which simulates composting processes under controlled conditions for 12 weeks. This is an important step in the analysis scheme to assess the compostability of plastic materials. The procedure consists, in short, of studying the differences found in plastics before and after subjecting them to the action of natural microbes found in compost. Although the use of natural fibers for composites obtaining has been widely studied in the literature, not much research has been conducted on the bio-disintegration behavior of such materials. So, the main aim of this paper is to determine if the introduction of cellulosic fibers into the polymer matrixes

modifies its susceptibility to the microorganisms' action and, thus, its disintegration.

Materials and Methods

Materials

A general-purpose PE from Matrix (Revolve N-461, Northampton, UK), in powder form, was used as matrix. The polylactic acid (PLA) matrix used was from Corbion (Luminy L105, with 99% L-isomer), also in powder form.

The fibers were obtained at Universidad de Las Palmas de Gran Canaria (ULPGC), following previously described processes [24]. In short, the extraction process consisted of a mechanical step of subsequent crushing of the stems. Once obtained and dried, fibers were cut to 3–4 mm in length. Part of these fibers was treated to improve thermal stability using a 1 N NaOH solution and a solid/liquid relation of 25 g/l. The treatment lasted 1 h at room temperature and ended with various washings with de-ionized water until reaching neutral pH. Untreated fibers showed an average diameter of $132 \pm 33 \mu\text{m}$, while for treated ones, this was $92 \pm 21 \mu\text{m}$.

Methods

Composites Production

Arundo fibers were dried overnight in an oven at 105 °C, while PE was dried at 40 °C overnight and PLA at 100 °C for 4 h. Composites were prepared by dry blending of the matrix with the fibers (at 5 and 10% weight) in a V-shape mixer and then introduced in a lab-made rotomolding device, as described previously [21], using a rotation rate of 2.30 rpm in the primary axis and 9.14 rpm in the secondary axis (speed ratio of 1/4). The internal air temperature in the mold was monitored with a thermocouple introduced via the venting hole located in the middle of one side of the cube. The heating stage stopped when the internal temperature reached 180 °C for PE and 185 °C for PLA, although due to thermal inertia, interior air temperature reached slightly higher values. The mold was cooled by forced air while keeping the mold rotation until reaching 50 °C. Average heating times were 22 min for PE and 32 for PLA, regardless of the incorporation of fibers. Contrarily, cooling times varied for PE samples; cooling was faster for 10% loadings than for 5% and pure PE (process cycles are found in supplementary materials (Fig. S1)). Cubic parts of 120 mm side and 3–4 mm thickness were obtained (Fig. 1), and test bars were machined from them, following ISO 3167:2014 standard for the dimensions of the test bars for tensile tests, ISO 178:2019 standards for flexural tests, and ISO 180:2019 standards for Izod-impact tests.

The samples obtained have been named with the matrix used (PE, PLA) followed by the type of fiber (AD: *Arundo donax*, ADt: *Arundo donax* treated) and the ratio of fiber (5, 10).

Fibers are well distributed in all composite parts obtained, although some clustering can be observed for 10% treated fibers, especially on the inner surface of the cubes (Fig. 1b, d–f). Untreated fiber does not seem to degrade during the processing, as the composites obtained do not show big bubbles, dark color, or characteristic odor. Some authors have experienced processing issues when using other fibers in rotomolded parts. For example, 10% hemp fiber composites did not even show enough consolidation unless using treated fibers [50]. However, in this research, *Arundo* fibers were successfully incorporated into the matrix, not forming fiber balls inside the part due to the mold rotation.

Bio-disintegration and thermal behavior were assessed for neat matrix and composites with 10% fibers.

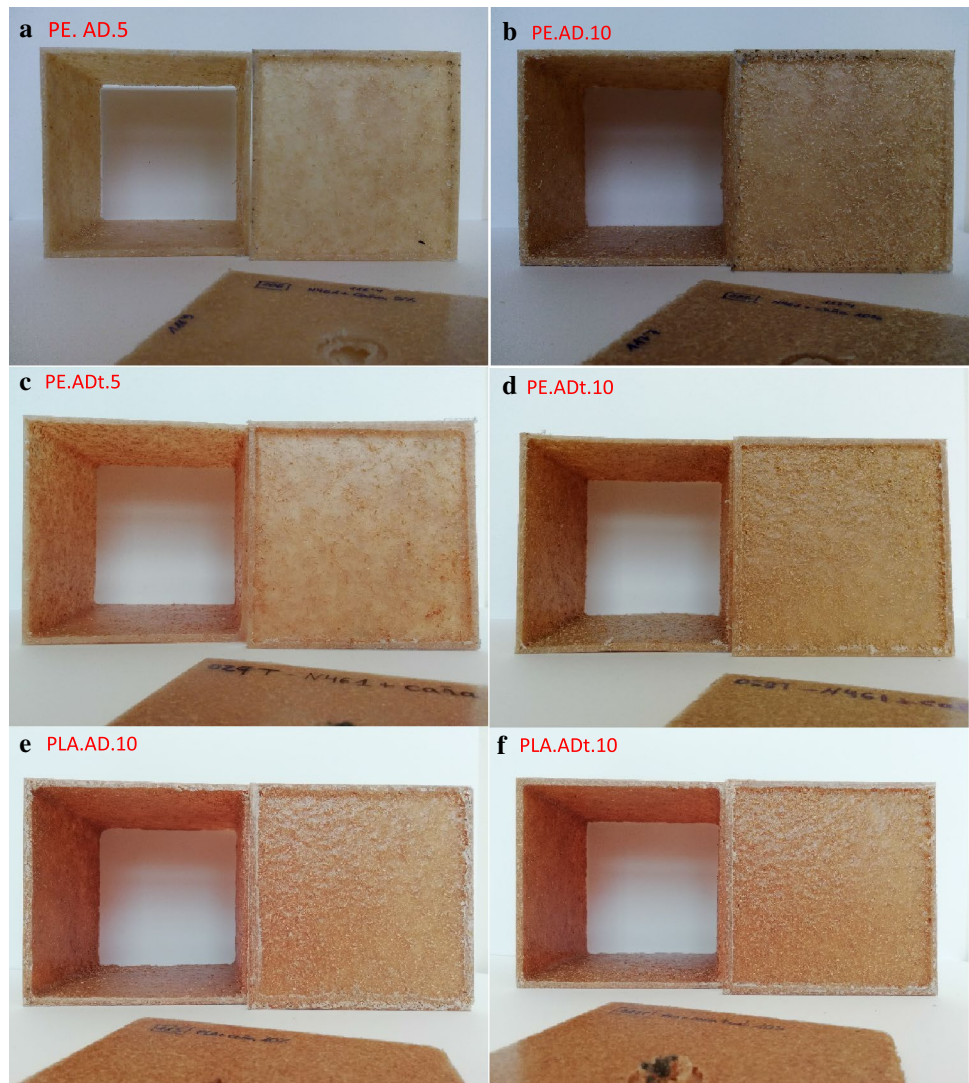
Mechanical Testing

Composite samples were tested to determine their tensile properties according to ISO 527–2:2012, at a rate of 10 mm/min, determining the elastic modulus and ultimate tensile strength. Flexural properties were measured according to ISO 178:2019 at the same rate, with a distance between cantilevers of 64 mm, determining the elastic modulus and flexural strength. Tensile and flexural tests were performed in a universal testing machine from Dongguan Liyi Test Equipment Co. Ltd. (LY-1065). A PCE-FG1k load cell of 200 kg maximum capacity from PCE Instrument) was used for the flexural tests, and a YZC-516 with 500 kg maximum capacity from Guang CE for the tensile essays. Impact tests were performed on unnotched samples, following UNE-EN ISO 180:2019, using a 5.5 J pendulum and an impact rate of 3.5 m/s. The energy absorbed by the part on Izod configuration was determined in an Izod and Charpy impact tester model LY-XJJD 50 from Dongguan Liyi Test Equipment Co. Ltd.

Bio-disintegration Assays

Disintegrability of the materials was determined by an assay performed in simulated composting conditions, following the protocol established in EN 14806:2005. A synthetic biowaste was prepared by mixing vegetal residues, rabbit feed (commercial product based on alfalfa and vegetable flours, with proteins and cellulose content of 15% and 20%, respectively), mature compost, volumizing agent (wood chips), urea and water (up to 55% of the final weight). This biowaste was placed in boxes (45 × 62 × 18 cm) with holes on the lower part and sides, set at 6.5 cm from the bottom.

Fig. 1 Pictures of composite parts obtained. PE composites with **a** 5% untreated fibers in PE, **b** 10% untreated fibers in PE, **c** 5% treated fibers in PE, and **d** 10% treated fibers. PLA composites with **e** 10% untreated fiber in PLA and **f** 10% treated fiber in PLA



A 5 cm—layer of expanded clay is placed on the bottom of the boxes to ensure ventilation and drainage.

The boxes are manually aerated weekly for the first four weeks and then every two weeks. pH, weight, and humidity levels were assessed weekly during the entire process, while temperatures were checked daily. Once dried and weighted, each sample was placed in the synthetic waste with enough distance not to touch either the walls of the box or other sample and then entirely covered with more synthetic waste. The overall duration of the assay was 12 weeks.

At the end of the test, the samples were recovered, washed with water, and oven-dried at 105 °C, obtaining the disintegration degree as follows:

$$\text{Disintegration degree (\%)} = \frac{m_f - m_o}{m_o} \cdot 100$$

where m_f is the dry mass of each test bar at the end of the assay and m_o is the initial mass of this same bar.

Microscopic Observations

After the tensile test, the surface of obtained parts and cross-section of test samples were observed under an optical microscope and SEM. An Olympus BX51 microscope was used for optical microscopy to assess the differences found in the parts' surfaces.

The surface microstructure of samples was also assessed before and after the disintegration assay. A Hitachi TM3030 tabletop scanning electron microscope (SEM) under different magnifications, working at 15 kV, was used for this purpose. Test bars were sputtered with a thin Au/Pd layer in an SC 760 apparatus from Quorum Technologies for 120 s and 18 mA under an argon atmosphere. For the assays after the bio-disintegration assay, PE samples were obtained by

cutting a layer of the test bars. For PLA, this was not possible due to the material fragility. These samples were then obtained just by pressing the samples with fingers.

Thermal Behavior

Differential scanning calorimetry (DSC) was performed on all samples in a Perkin Elmer DSC 4000 apparatus. The measurements were performed at 10 °C/min, from 30 to 200 °C, with two heating cycles. Melting temperature for both heatings (T_{m1} and T_{m2} , respectively) and crystallization temperature (T_c) from the cooling step were determined, together with melting and crystallization enthalpies (ΔH_{m1} , ΔH_{m2} , and ΔH_{cc}). Cold crystallization temperature (T_{cc}) was not observed for the studied samples. For PLA samples, glass transition temperature (T_g) was also calculated. Enthalpies were used for crystallinity degree (χ) calculation, using the following expression:

$$\chi = \frac{1}{1 - m_f} \cdot \frac{\Delta H_m - \Delta H_{cc}}{\Delta H_0} \cdot 100$$

where ΔH_0 is the enthalpy for 100% crystalline sample (93.7 J/g for PLA and 293 J/g for PE) [17], and m_f is the mass fraction of the fiber (10% for composites). Three assays were performed for each sample, and results are given as average values and standard deviations.

Infrared Spectroscopy (FTIR)

Fourier infrared spectra of the samples were recorded in the range of 400–4000 cm^{-1} in a Perkin Elmer Spectrum Two spectrometer, in the attenuated total reflection mode (ATR), with a resolution of 4 cm^{-1} . Different intensity ratios were

calculated for each polymer matrix to determine the extension of the sample changes. Three spectra were obtained for each sample, accumulating 60 scans per spectrum.

Results

Evolution of Bio-disintegration Recipients

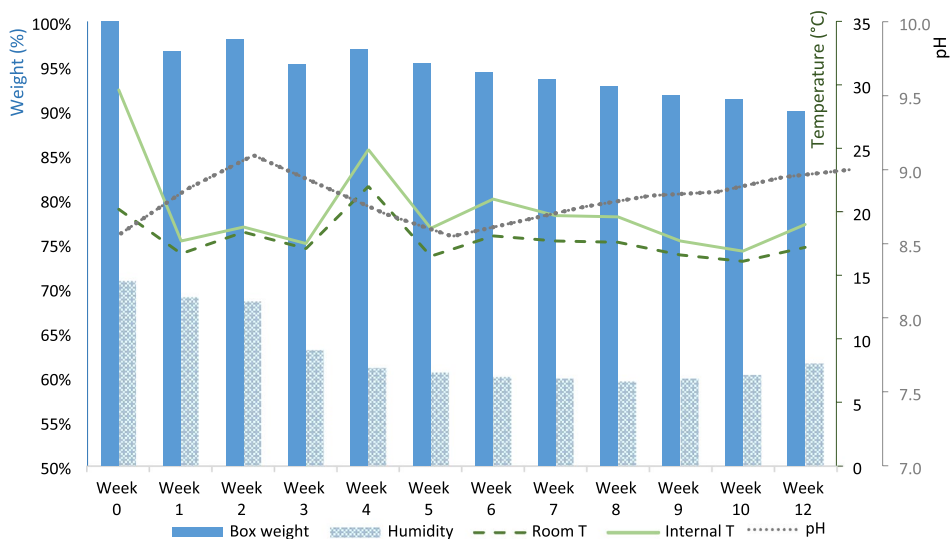
The variation of the magnitudes measured during the entire assay is drawn in Fig. 2: the weight of the disintegration boxes (in %), temperature, and humidity values.

It is clearly observed that the weight is reduced gradually, due mainly to the reduction in the humidity of the synthetic biowaste, as also observed in the figure. Initial pH was 8.31, which increased during the first weeks, coinciding with the release of ammonia odor, which was later disappearing, as expected. The maximum pH value was 9.1 in week 4. No signs of mold or other alterations were observed during the process.

The graph also shows that the biowaste temperature is progressively decreasing due to the low biological activity. In any case, the temperature inside the disintegration boxes was higher than the room temperature, and condensation could be observed on the recipients' walls, thus indicating the existence of biological activity inside them. Room temperature was quite variable in the period of the year where the assay took place (March–May). Some more mature compost and vegetable residues were added to the biowaste to increase the microbial activity and overcome this instability, although this did not have much effect (this is the reason for the weight increase in week 4).

At the end of the assay, the biowaste did not have any specific odor, and its color was notably darker. Photographs

Fig. 2 Evolution of weight and humidity in the disintegration boxes (left axis), together with temperature and pH (right axis)



of the samples were taken for visual comparison and also observed in an optical microscope. Some samples (PLA composites) were broken when recovered.

Recovered samples were dried and weighted to determine the extent of the disintegration as the weight loss percentage. Figure 3 shows that the PE samples have almost no change, while weight loss of up to 1.4% for PLA composites was obtained. 100% PLA samples do not show a significant disintegration, while adding natural fibers seems to increase this behavior slightly. It should be pointed out that, to verify that the assay was correctly prepared and that biological activity existed, a commercial biodegradable material (Bioplast 300, based on starch) was introduced as reference material, and this reached almost 40% in weight reduction. As already mentioned, PLA is considered compostable in thermophilic conditions, which is, at around 60 °C, which explains the low values of weight loss obtained in this study. Other authors working in compost piles at similar temperatures have also got similar weight losses [51]. The crystallinity of the PLA also plays a vital role in the disintegration and degradation behavior. As shown later, the grade used in this research showed high crystallinity (around 50%), which could also explain the relatively low degradation. The PLA grade used contains 99% of L-isomer, also influencing the degradation; the higher D—enantiomer content, the higher degradation rates, and the lower crystallinity (also increasing degradation kinetics) [48].

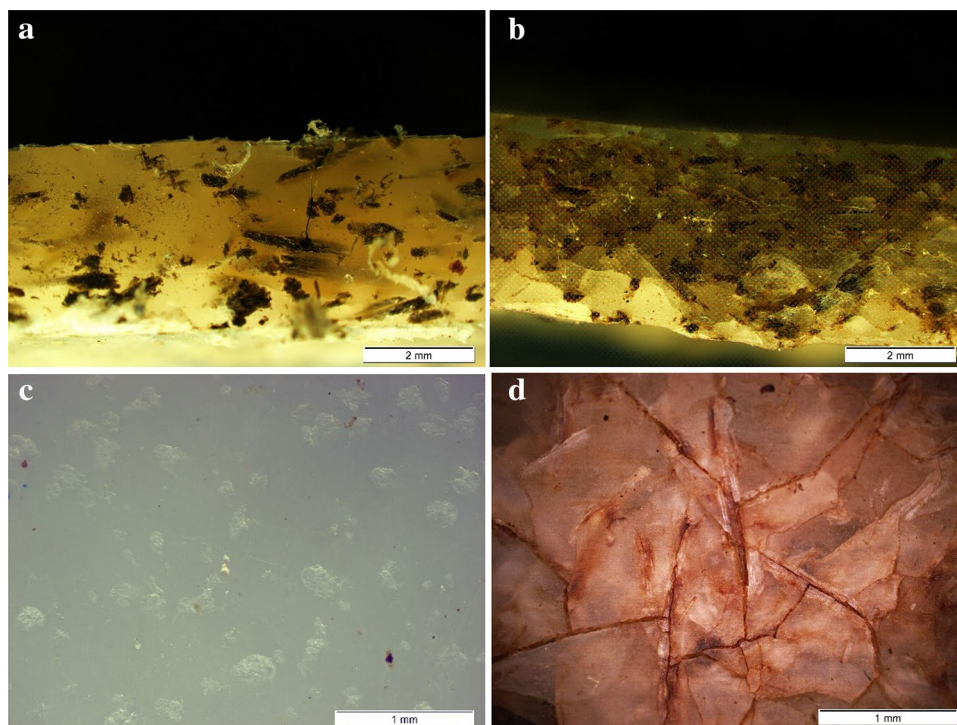
The increase in the hydrophilicity of the composite is needed for PLA degradation; for that reason, the

introduction of vegetal fibers could help in the PLA hydrolysis reactions [51, 52]. For this reason, the humidity absorption of samples before and after the process was measured (Table 1). As observed, humidity absorption of samples before the process is almost null (maximum around 1% for PLA composites), while this increased to close to 20% for PLA-treated *Arundo* composites. PE composites increase their hydrophilicity after the disintegration assay, reaching around 5% of moisture absorption. Before bio-disintegration, the hydrophilicity of PE and PLA composites is higher than for neat polymers, regardless of whether the fiber has been or not treated; due to the nature of the polymer, PLA materials show higher moisture absorption than PE-based ones. However, the PLA parts with treated fibers show significantly higher hydrophilicity than untreated ones after the essay,

Table 1 Average values (\pm standard deviations) for disintegration degree and moisture absorption

Material	Disintegration degree (%)	Moisture absorption (%)	
		Before	After
PE	0.11 \pm 0.03	0.09 \pm 0.03	0.86 \pm 0.31
PE.AD 10	- 0.58 \pm 0.07	0.90 \pm 0.10	4.66 \pm 0.23
PE.ADt 10	- 0.72 \pm 0.04	0.90 \pm 0.06	5.88 \pm 0.30
PLA	- 0.30 \pm 0.10	0.68 \pm 0.03	4.03 \pm 0.55
PLA.AD 10	- 0.89 \pm 0.07	1.27 \pm 0.04	12.63 \pm 0.45
PLA.ADt 10	- 1.40 \pm 0.28	1.32 \pm 0.04	19.11 \pm 0.88

Fig. 3 Optical microscope pictures taken after the disintegration assay. Lateral view of composites: **a** 10% *Arundo* in PE matrix, **b** 10% *Arundo* in PLA matrix, **c** Surface of PLA, **d** Surface of 10% *Arundo* PLA



which correlates with the higher disintegration degree. The moisture absorption of PE composites increases after the essay and is significantly higher than for PE, but fiber treatment does not show any statistical difference.

Regarding the extent of the disintegration, PE materials do not show differences among the three series of materials tested; that is, no breakdown happens for this matrix. The increase in hydrophilicity is then only due to the presence of fibers in the matrix. On the other hand, the introduction of giant reed fibers within the PLA matrix increases the biodegradation ability of the material, especially for NaOH-treated fibers. Dong et al. [53] have found a similar behavior for PLA/coir composites obtained by compression molding; parts with treated fibers provide higher disintegration rates in soil burial assay. These authors attribute this behavior to the release of residual NaOH and its interaction with the polymer chain. This paper also points out that a fiber ratio over 10% does not lead to further increases in biodegradability kinetics. The increase in weight loss for PLA composites compared to neat PLA can be due to their higher hydrophilicity and the higher porosity obtained for these composites, which increases the surface exposed to water and the biota in the synthetic waste.

Mechanical Properties

Table 2 shows a summary of results obtained for the different properties assessed. The composite density is lower than the density obtained for the polymer parts. The fiber treatment does not significantly affect the density of the composite, being more relevant the amount of fiber in the material. Other authors have reported a higher density of the composite for treated fiber composites than for untreated ones [21, 54]. As fibers used in this research have similar composition [24] to those obtained by Fiore and collaborators [23], the density determined by these authors (1.168 g/cm³) can be assumed. Comparing composites' theoretical

density (density of the polymer and density of the filler multiplied by the ratios of each component) with the actual one (obtained by volume and weight measuring of the samples), calculating the porosity of the different materials. Higher fiber loadings result in higher porosity values. Besides, the use of treated fibers also led to an increase in porosity due to the formation of fiber agglomerations and poorer distribution, although this does not seem to affect the mechanical properties of the composite. This higher porosity, also observed in microscopy, is responsible for the relatively low mechanical properties determined.

Neither for PE nor for PLA composites did the NaOH treatment performed on the fibers seem to affect the mechanical properties of the composites, contrary to what was expected, being more significant the amount of fiber used, as also happened for density.

For PE, the impact strength is only significantly reduced for composites with 10% fibers, with no significant difference due to the fiber treatment. 5% PE composites show no statistical differences for this property for untreated and treated fibers. Longer fibers can provide better impact properties, as the energy needed for fiber pull-out is higher due to the longer distance required for this to happen [55] (assuming fiber does not break). However, in rotational molding, particle size distribution is a critical aspect for obtaining a well-consolidated part [54]; besides, long fibers result in entanglements, poor distribution, and the fibers not incorporated into the polymer matrix [50, 56]. The low impact properties found in this research have been previously reported in the literature for rotomolded composites [15, 16, 57] and can be explained by the low adhesion between the matrix and the fiber. Ortega et al. have obtained composites with up to 20% of size-classified *Arundo* fibers in a rotomolded PE matrix, also finding significant drops in impact strength [21]. Some authors have proposed using compatibilizers based on maleic anhydride to increase this adhesion and thus the composite efficiency [55]. The production of parts with different

Table 2 Average values (\pm standard deviations) for mechanical properties of the materials

Material	Density (g/cm ³)	Impact Strength (kJ/m ²)	Tensile properties		Flexural properties		Porosity (%)
			Strength (MPa)	Modulus (MPa)	Strength (MPa)	Modulus (MPa)	
PE	0.901 \pm 0.023	19.0 \pm 3.8 ^d	16.1 \pm 0.3	381.5 \pm 59.4	18.7 \pm 2.1 ^l	623.7 \pm 75.2 ⁿ	3.6
PE.AD 5	0.855 \pm 0.013 ^a	15.4 \pm 3.4 ^d	13.4 \pm 0.4 ^g	467.7 \pm 33.8 ^j	18.2 \pm 1.4 ^l	662.8 \pm 112.5 ⁿ	6.5
PE.AD 10	0.809 \pm 0.031 ^b	11.8 \pm 4.7 ^e	11.4 \pm 0.8 ^h	489.0 \pm 32.9 ^j	18.3 \pm 0.7 ^l	791.6 \pm 115.2 ⁿ	12.8
PE.ADt 5	0.838 \pm 0.340 ^a	14.7 \pm 3.4 ^d	13.4 \pm 1.4 ^g	544.7 \pm 81.4 ^j	18.1 \pm 1.1 ^l	690.1 \pm 105.7 ⁿ	8.3
PE.ADt 10	0.804 \pm 0.170 ^b	9.8 \pm 1.8 ^e	11.8 \pm 0.8 ^h	502.6 \pm 81.4 ^j	17.3 \pm 1.0 ^l	737.9 \pm 125.9 ⁿ	13.3
PLA	1.212 \pm 0.024	21.1 \pm 5.0	17.3 \pm 5.6 ⁱ	865.4 \pm 161.5 ^k	57.7 \pm 4.5	3862.1 \pm 412.1 ^o	2.3
PLA.AD 10	1.088 \pm 0.024 ^c	4.0 \pm 1.4 ^f	20.1 \pm 2.7 ⁱ	874.0 \pm 179.0 ^k	33.7 \pm 2.6 ^m	3148.3 \pm 280.0 ^o	10.1
PLA.ADt 10	1.079 \pm 0.037 ^c	3.7 \pm 0.7 ^f	18.5 \pm 2.8 ⁱ	774.8 \pm 108.4 ^k	33.4 \pm 6.3 ^m	3007.3 \pm 690.2 ^o	10.6

Tukey tests for comparison of properties of the different series of materials have been used at a 95% confidence level.

Those materials with the same superscript letter show no statistical difference for the property.

layers, at least one of them the neat polymer, has also been proposed as a strategy to reduce the drop in impact properties [8, 15]. However, this requires higher processing times, makes the process more complicated, and reduces the fiber ratio in the final part.

Tensile strength is diminished for all samples, being this loss more important for higher percentages of fibers. Other works working with lignocellulosic materials in rotational molding have also found lower tensile strength with increased fiber content [1, 20, 21, 58]; tensile strength drops by 50% when working with as low as 5% of hemp fibers [50]. This reduction may be due to the increased porosity of samples with the fiber introduction and the fiber agglomeration, which limits stress transfer between the fibers and the matrix.

Tensile elastic modulus slightly increases for the PE-composites, with no difference in this case due to the fiber content. It is accepted that the introduction of fibers will increase tensile modulus due to their higher rigidity [55]. In any case, the particularities of the rotational molding process, where no pressure is applied, result in lower increases for this property than in other procedures, such as injection or compression molding [16]. Using compatibilizers based on maleic anhydride results in higher tensile modulus [55].

Finally, no significant changes in flexural properties are found among neat PE and composites, despite the ratio of fiber used. Other studies have found no differences in these properties when using 10% bamboo [57] or agave fibers [55].

For PLA, the impact strength is greatly reduced due to fibers, reaching around 20% of the values found for the polymer, for composites with treated and untreated fibers. This drop, together with the reduction to almost half in flexural strength, can be attributed to the increased porosity of the samples and the pull-out of the fibers from the matrix, as already explained for PE. Incorporating *Arundo* fibers in the PLA matrix has not modified the tensile properties of PLA. Similarly, agave fibers have not significantly changed tensile properties in PLA [16]. In contrast, using buckwheat husk in lower proportions has led to a drastic decrease in tensile strength [17] at comparable porosity values. This difference in behavior may be due to the format of the material used in both studies (fibers here and particles in that study), as it is well known that the morphology of the filler affects the reinforcing effect.

Microscopic Observations

Optical microscope pictures allowed observing some porosity and voids in the parts, even before the disintegration process. Good distribution of fibers is found along the surface and through the wall thickness of the specimens (Fig. 3). The only change observed in PE parts is the darkening of the fibers, while for PLA ones, many cracks appear in the surface

and cross-section of the parts. Pure PLA parts show some more roughness on the surface after the assay, although no cracks are visible (pictures of the samples before the assay are found in supplementary material (Fig. S2)). The swelling of fibers during the process may have forced the cracks to appear by size increase or by the water effect in the PLA and the beginning of hydrolysis.

The cracks appearing in PLA composite (Fig. 3b, d) parts were visible to the naked eye when recovering the parts from the synthetic compost. Some of them were even broken after the process, thus showing the extent of the degradation that occurred, even for the low weight loss observed in the assay and previously discussed.

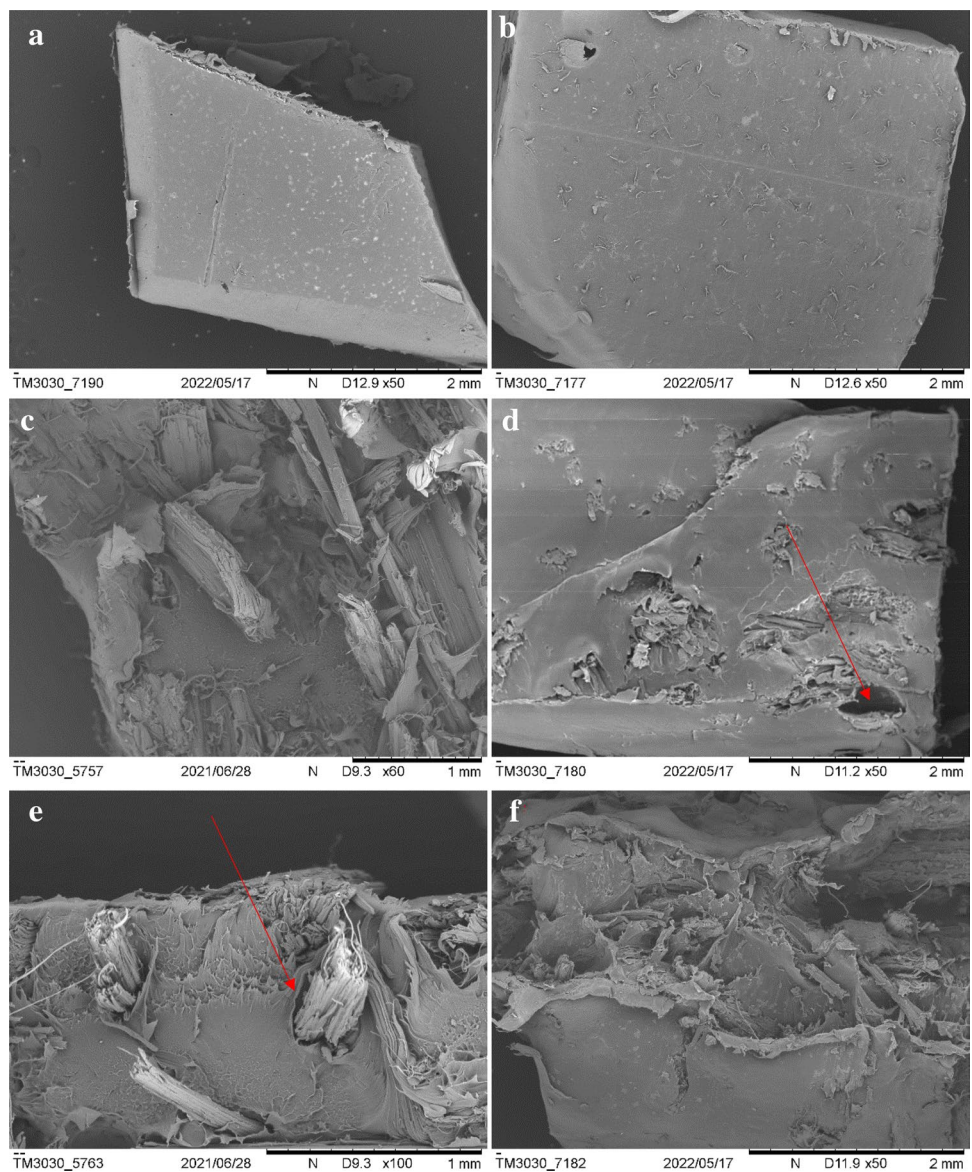
SEM micrographs for PE and PLA samples (Figs. 4, 5, respectively) show a smooth surface, almost free of porosity, while some voids can be observed for composites. For both matrixes, fibers appear randomly distributed and with poor adhesion with the matrix, as pull-out and separation between fiber and matrix are observed, thus explaining the relatively poor mechanical properties of the prepared composite. As already mentioned, no differences were found in SEM observations due to the bio-disintegration assay for this matrix. For PLA, however, the material appears fragmented, with many cracks on all surfaces of PLA-composite parts, as also observed in the optical microscope.

DSC

Typical DSC curves and results are obtained for all composites before and after the disintegration assay, as observed in Table 3 for PE samples and Table 4 for PLA ones. For polyethylene samples, the melting temperature is around 129 °C, with no difference due to the fiber content. No difference in temperatures due to the bio-disintegration assay was found, indicating, once again, that the biological process does not modify these materials. Melting and crystallization peaks are not altered, and enthalpies are only slightly reduced due to fiber introduction. Finally, no differences between the first and second heating cycles were observed, neither in temperatures nor in crystallinity values (values not shown in Table 2). Crystallinity seems to decrease in the assay because of the differences in melting enthalpies, which are also lower. This apparent reduction in crystallinity might be confirmed by other techniques, such as X-ray diffraction. Other authors have reported similar behavior for PE composites: no significant differences in thermal properties when adding foreign materials and crystallinity levels of around 40% due to the rapid crystallization of PE [17].

For PLA samples (Table 4), glass transition (58 °C) and melting temperatures (170 °C) are placed within the ranges indicated by the product datasheet and are also similar to other PLA-based materials. T_g increases with the introduction of *Arundo* fibers due to hindering PLA chains' mobility

Fig. 4 SEM micrographs for PE samples. Left pictures correspond to samples before disintegration assay, right ones, after. **a, b** PE, **c, d** PE + 10% *Arundo* fibers, **e, f** PE + 10% treated *Arundo* fibers

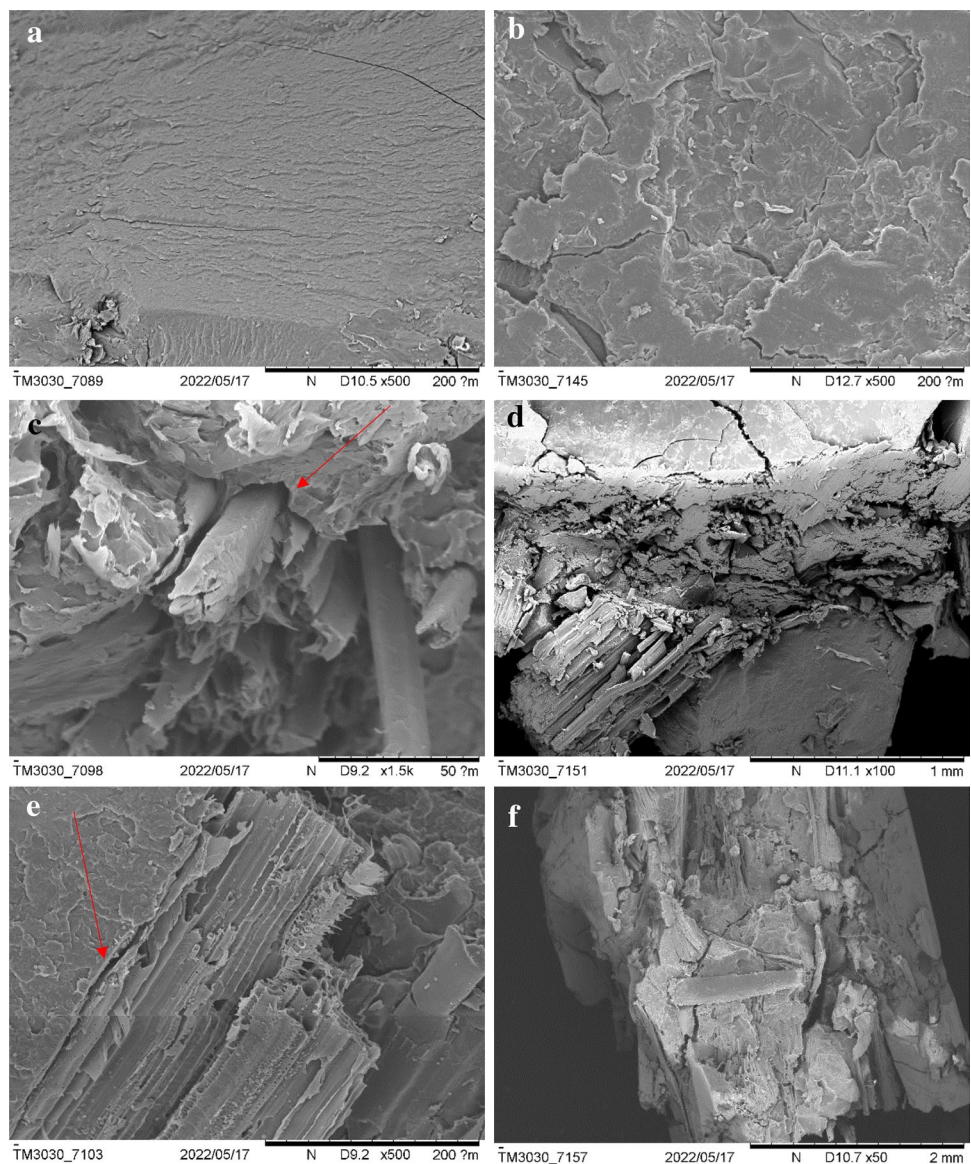


[16]. This is also observed here for T_m , which may indicate that the PLA matrix did not suffer any degradation during the processing. No cold crystallization is observed, probably because a high crystallinity level can be obtained from the process, due to the long cycle time, especially in the cooling stage. Other authors [17] found lower crystallinity values in this same process, although with a different PLA grade, also observing increases in this parameter with the introduction of lignocellulosic materials and finding a cold crystallization band. A crystallization peak in the cooling stage is observed for all samples, contrary to what was observed by Andrzejewski et al. in their mentioned work. However, other authors obtaining high crystallinity levels for the neat PLA have also observed a decrease in crystallinity when introducing foreign materials [59], thus showing the dependence of crystallinity levels with the PLA grade and the filler/

reinforcement used. Greco et al. [4] have demonstrated that rotomolded PLA after aging for 60 days at room temperature does not show any cold crystallization peak, which is in line with observations in this study, where DSC was performed not immediately after parts obtaining. So, *Arundo* fibers may act in this paper not as a nucleating agent but as hindering the crystallization naturally occurring for this material.

Once more, PLA samples show significant changes in the thermal behavior because of the assay. The melting and glass transition temperature decreased in the samples after the biological assay. This may indicate a reduction of the average molecular weight of the polymer and, thus, that the assay affects (degrades to some extent) the matrix. The composites show higher reductions than the neat PLA samples, which means that the introduction of fibers positively impacts the material's disintegration. This is probably due to the higher

Fig. 5 SEM micrographs for PLA samples. Left pictures correspond to samples before disintegration assay, right ones, after. **a, b** PLA, **c, d** PLA + 10% Arundo fibers, **e, f** PLA + 10% treated Arundo fibers



water absorption found for composite samples, as moisture has been determined as a determinant factor in the biodegradation process.

Table 3 Thermal parameters for PE samples from DSC assays

Material	T_{m1} (°C)	T_{m2} (°C)	T_c (°C)	χ_1 (%)
Before the disintegration assay				
PE	129.0 ± 0.5	127.0 ± 0.1	109.9 ± 0.2	41.4 ± 0.8
PE.AD	129.6 ± 0.4	128.4 ± 0.3	108.2 ± 0.2	34.3 ± 5.3
PE.ADt	129.1 ± 0.1	127.2 ± 0.0	109.7 ± 0.0	38.1 ± 5.6
After the disintegration assay				
PE	129.3 ± 0.9	128.5 ± 0.8	108.5 ± 0.7	30.6 ± 2.5
PE.AD	129.7 ± 0.1	126.8 ± 0.0	109.9 ± 0.0	37.9 ± 0.5
PE.ADt	131.3 ± 1.2	128.3 ± 0.6	108.5 ± 0.8	31.7 ± 3.2

The second heating curve for samples after the disintegration assay shows a double melting peak, not appearing in the first heating. This can be explained by the first thermal heating, where the PLA thin crystals' are able to melt and recrystallize at low heating rates, the existence of more than one crystal structure, or the presence of different lamella morphologies [38]. This ability to crystallize can be seen in the second heating cycle, which continues showing high crystallinity levels.

FTIR

FTIR spectra for PE samples show no variations among the fingerprint of pure PE or composites (Fig. 6), thus meaning the polymer fully covers the fibers. The main differences are a wide band (low intensity) between 3600

and 3000 cm^{-1} and the appearance of small bands between 1200 and 900 cm^{-1} , which are attributed to the presence of fibers. For samples after the disintegration assay, these differences are even less noticeable. If the spectra before and after the assay are compared, no differences are found, thus evidencing, once again, the low effect of the assay on the properties of the composite. Some works studying the aging of PE point out the appearance of some peaks in the FTIR spectra related to carbonyl, peroxides, and unsaturated groups at around 1700 , 1200 , and 900 cm^{-1} [60], while differences in the intensities at 2920 , 1465 and 717 cm^{-1} are indicative of degradation [61]. The evaluations performed in this work have not found any of these

bands for PE, meaning none of these groups are present in the samples, or at least not in a noticeable proportion.

On the other hand, for PLA samples, no difference is observed with the introduction of fibers in the matrix (Fig. 7). At the same time, some evident changes can be seen when comparing the spectra before and after the disintegration assay, as peaks for fiber overlap those of PLA and because polymer mostly covers the fibers. So, no evident interaction between the fibers and the matrix is observed, as otherwise observed in SEM micrographs. These spectra show the typical bands for PLA, that is, carbonyl ($\text{C}=\text{O}$) stretch in lactide (1747 cm^{-1}), -CH_3 bend (1465 cm^{-1} , 1381 cm^{-1} , and 1127 cm^{-1}), C-O stretch (1180 , 1078 and 1043 cm^{-1}). Bands at 866 and 756 cm^{-1} are related,

Table 4 Thermal parameters for PLA samples from DSC assays

Material	T_{m1} ($^{\circ}\text{C}$)	T_{m2} ($^{\circ}\text{C}$)	T_c ($^{\circ}\text{C}$)	χ_1 (%)	χ_2 (%)	T_g ($^{\circ}\text{C}$)
Before the disintegration assay						
PLA	170.4 ± 1.4	167.3 ± 3.0	109.0 ± 0.4	61.9 ± 5.5	52.1 ± 10.8	58.1 ± 0.7
PLA.AD	174.5 ± 2.7	172.9 ± 4.5	108.4 ± 1.6	45.6 ± 3.0	41.5 ± 8.8	67.7 ± 1.2
PLA.ADt	175.7 ± 0.4	175.2 ± 0.1	110.1 ± 0.1	40.2 ± 2.4	36.4 ± 0.2	68.9 ± 0.1
After the disintegration assay						
PLA	168.5 ± 1.8	163.1 ± 2.5	107.2 ± 3.6	57.7 ± 12.3	48.0 ± 9.0	59.1 ± 2.8
PLA.AD	170.3 ± 1.4	164.4 ± 0.7	109.9 ± 0.2	48.7 ± 2.5	48.9 ± 3.0	62.9 ± 0.4
PLA.ADt	168.2 ± 0.1	159.2 ± 4.7	107.4 ± 2.0	59.9 ± 6.9	55.7 ± 8.6	63.6 ± 3.0

Fig. 6 FTIR spectra for PE samples before the disintegration assay (left) and after (right)

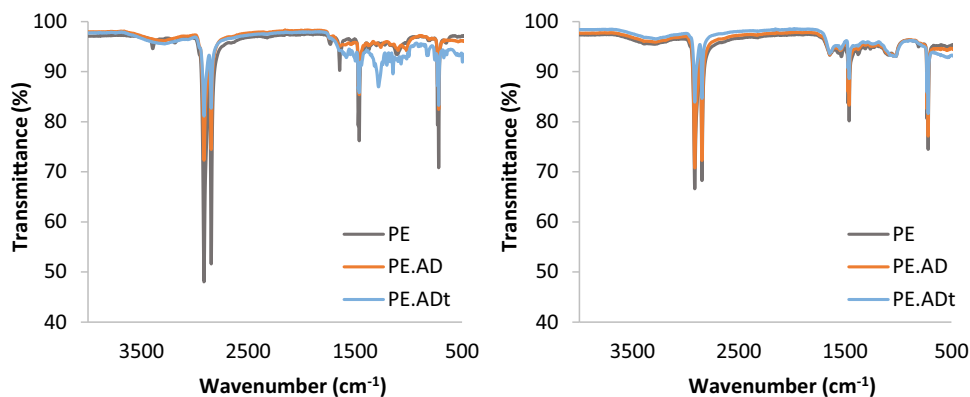
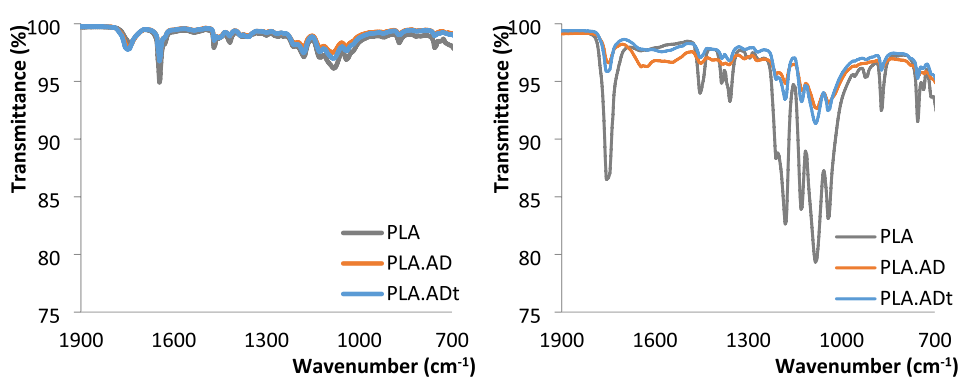


Fig. 7 FTIR spectra for PLA samples before the disintegration assay (left) and after (right)



respectively, to the amorphous and crystalline phases of PLA [11, 62]. Gorrasi et al. also propose using the band at 920 cm^{-1} as an indicator of crystallinity [48].

To determine the degradation extent, the bands related to carbonyl groups and ester groups are of particular interest because the degradation of the matrix can lead to the formation of anhydrides, carbonyl, and carboxyl groups. Some ratios are calculated with the absorption values for these bands, using the band for $-\text{CH}_3$ to normalize results [11, 52]. Table 5 shows the absorption values for these bands and the ratios obtained by dividing them by this at 1465 cm^{-1} . Ratios 1–3 (related to disintegration) show a significant increase in the comparisons before and after the disintegration assay, showing the extent of the modifications in the materials. For R4, related to the sample crystallinity, no trend is observed, which otherwise correlates with the DSC results on this parameter; this same observation is made when comparing the peaks at 922 cm^{-1} . On the other hand, higher ratios are also observed for composites than for neat PLA, as these refer to carboxyl and ester groups, also present in fibers.

Conclusion

Arundo donax fibers from stems have been introduced into rotomolded PE and PLA matrixes following a simple dry blending method, obtaining acceptable porosity levels and good fiber distribution. The impact properties are greatly affected by introducing 10% of fibers for both matrixes. PE composites show similar flexural behavior to pure PE, with a decrease of around 15% in tensile strength and an increase of over 20% in elastic modulus. PLA composites show similar properties to neat PLA, except for a significant decrease (around 40%) in flexural strength. The relatively poor mechanical behavior of the composites can be explained by the presence of voids and the poor adhesion between fiber and matrix, as found in SEM observations. NaOH fiber treatment does not affect the composite's mechanical or thermal properties.

Regarding the bio-disintegration assays, PE is almost unaffected, as no changes in FTIR spectra, calorimetric behavior, or morphology features are found. The composite after the assay seems to be slightly more hydrophilic and has less crystallinity. On the other hand, modifications to PLA-based materials are visible just after recovering the samples from the synthetic residue prepared. For these parts, many cracks are observed, especially for composite samples. The degradation is confirmed in DSC assays, with a reduction in glass transition and melting temperatures. FTIR analysis also shows the degradation of the matrix, with the increase in the intensity of bands related to carbonyl and ester groups; some ratios calculated for these peaks and normalized show the extent of the modifications achieved. The treated fiber composites show higher values for these ratios, which the presence of residual alkali solution may explain.

The weight loss of the samples during the bio-disintegration assay is almost null for the PE samples, being also quite low for the PLA samples. This can be explained by the low temperature used in the process and the characteristics of the PLA grade used in this work, with high crystallinity and L-isomer.

The greater extent of modification found for PLA composites compared to neat PLA can be explained by the higher water absorption due to the natural fibers' addition, which is an essential step for PLA degradation. Further assays should be performed to determine the changes in the polymer matrix, for example, if PLA has reduced its average molecular weight. Besides, the crystallinity of samples using X-ray diffraction could also help understand how the incorporation of fibers affects the crystallinity of these composites and if this is modified during the bio-disintegration process. Finally, micro-CT could also be performed before and after the assay to determine changes in porosity.

This paper shows the extent of the modifications that occurred in lignocellulosic fibers/PLA composites in a low-temperature disintegration process, as a first approach to determining the biodegradability of these materials.

Supplementary Information The online version contains supplementary material available at <https://doi.org/10.1007/s10924-022-02542-x>.

Table 5 Absorption ratios for characteristic bands in PLA degradation

Material	R1 = 1747/1465	R2 = 1183/1465	R3 = 1085/1465	R4 = 756/866
Before the disintegration assay				
PLA	0.679	1.244	0.849	1.119
PLA.AD	1.043	1.252	0.925	0.970
PLA.ADt	2.064	2.503	2.108	1.030
After the disintegration assay				
PLA	2.702	4.030	3.324	1.124
PLA.AD	1.597	2.727	1.961	1.128
PLA.ADt	1.947	3.159	2.510	1.132

Author Contributions ZO, LS and MDM performed the study conception and design. Material preparation, data collection and analysis were performed by LS, FR, RP and ZO. ZO wrote the first draft of the manuscript, and all authors commented on its previous versions. All authors read and approved the final manuscript.

Funding Open Access funding provided thanks to the CRUE-CSIC agreement with Springer Nature. European Funding for Regional Development (FEDER) funded this research through the INTERREG MAC 2014–2020 program, providing funds for MAC Inv2Mac project (Grant number MAC2/4.6d/229). Luis Suárez also acknowledges the funding through the Ph.D. grant program cofinanced by the Canarian Agency for Research, Innovation and Information Society of the Canary Islands Regional Council for Employment, Industry, Commerce and Knowledge (ACIISI) and by the European Social Fund (ESF) (Grant number TESIS2021010008).

Data Availability The datasets generated or analyzed during the current study are available from the corresponding author upon reasonable request.

Declarations

Conflict of interest The authors report there are no competing interests to declare.

Open Access This article is licensed under a Creative Commons Attribution 4.0 International License, which permits use, sharing, adaptation, distribution and reproduction in any medium or format, as long as you give appropriate credit to the original author(s) and the source, provide a link to the Creative Commons licence, and indicate if changes were made. The images or other third party material in this article are included in the article's Creative Commons licence, unless indicated otherwise in a credit line to the material. If material is not included in the article's Creative Commons licence and your intended use is not permitted by statutory regulation or exceeds the permitted use, you will need to obtain permission directly from the copyright holder. To view a copy of this licence, visit <http://creativecommons.org/licenses/by/4.0/>.

References

- Hejna A, Barczewski M, Andrzejewski J et al (2020) Rotational molding of linear low-density polyethylene composites filled with wheat bran. *Polymers (Basel)* 12:1004. <https://doi.org/10.3390/POLYM12051004>
- Greco A, Maffezzoli A (2016) Rotational moulding of poly-lactic acid. *AIP Conf Proc* 1779:060007. <https://doi.org/10.1063/1.4965528>
- Greco A, Maffezzoli A (2017) Rotational molding of poly(lactic acid): effect of polymer grade and granulometry. *Adv Polym Technol* 36:477–482. <https://doi.org/10.1002/ADV.21630>
- Greco A, Ferrari F, Maffezzoli A (2019) Processing of super tough plasticized PLA by rotational molding. *Adv Polym Technol* 2019:1–8. <https://doi.org/10.1155/2019/3835829>
- González-López ME, Pérez-Fonseca AA, Manríquez-González R et al (2019) Effect of surface treatment on the physical and mechanical properties of injection molded poly(lactic acid)-coir fiber biocomposites. *Polym Compos* 40:2132–2141. <https://doi.org/10.1002/pc.24997>
- Ruiz-Silva E, Rodríguez-Ortega M, Rosales-Rivera LC et al (2021) Rotational molding of poly(Lactic Acid)/polyethylene blends: effects of the mixing strategy on the physical and mechanical properties. *Polymers* 13:217. <https://doi.org/10.3390/POLYM13020217>
- Vignali A, Iannace S, Falcone G (2019) Lightweight poly(ϵ -Caprolactone) composites with surface modified hollow glass microspheres for use in rotational molding: thermal, rheological and mechanical properties. *Polymers* 11:624. <https://doi.org/10.3390/POLYM11040624>
- Díaz S, Ortega Z, McCourt M et al (2018) Recycling of polymeric fraction of cable waste by rotational moulding. *Waste Manag* 76:199–206. <https://doi.org/10.1016/J.WASMAN.2018.03.020>
- Pick L, Hanna PR, Gorman L (2022) Assessment of processibility and properties of raw post-consumer waste polyethylene in the rotational moulding process. *J Polym Eng* 42:374–383. https://doi.org/10.1515/POLYENG-2021-0212/MACHINEREA_DABLECITATION/RIS
- Barczewski M, Hejna A, Aniśko J et al (2022) Rotational molding of polylactide (PLA) composites filled with copper slag as a waste filler from metallurgical industry. *Polym Test* 106:107449. <https://doi.org/10.1016/J.POLYMERTESTING.2021.107449>
- Aniśko J, Barczewski M, Mietliński P et al (2022) Valorization of disposable polylactide (PLA) cups by rotational molding technology: the influence of pre-processing grinding and thermal treatment. *Polym Test* 107:107481. <https://doi.org/10.1016/j.polymertesting.2022.107481>
- Cisneros-López EO, Pal AK, Rodríguez AU et al (2020) Recycled poly(lactic acid)-based 3D printed sustainable biocomposites: a comparative study with injection molding. *Mater Today Sustain*. <https://doi.org/10.1016/j.mtsust.2019.100027>
- Torres FG, Aragon CL (2006) Final product testing of rotational moulded natural fibre-reinforced polyethylene. *Polym Test* 25:568–577. <https://doi.org/10.1016/j.polymertesting.2006.03.010>
- Wang B, Panigrahi S, Tabil L, Crerar W (2007) Pre-treatment of flax fibers for use in rotationally molded biocomposites. *J Reinf Plast Compos* 26:447–463. <https://doi.org/10.1177/0731684406072526>
- Ortega Z, Monzón MD, Benítez AN et al (2013) Banana and abaca fiber-reinforced plastic composites obtained by rotational molding process. *Mater Manuf Process* 28:879–883. <https://doi.org/10.1080/10426914.2013.792431>
- Cisneros-López EO, Pérez-Fonseca AA, González-García Y et al (2018) Polylactic acid-agave fiber biocomposites produced by rotational molding: a comparative study with compression molding. *Adv Polym Technol* 37:2528–2540. <https://doi.org/10.1002/adv.21928>
- Andrzejewski J, Krawczak A, Wesoly K, Szostak M (2020) Rotational molding of biocomposites with addition of buckwheat husk filler. Structure-property correlation assessment for materials based on polyethylene (PE) and poly(lactic acid) PLA. *Compos Part B Eng* 202:108410. <https://doi.org/10.1016/j.compositesb.2020.108410>
- González-López ME, Pérez-Fonseca AA, Cisneros-López EO et al (2019) Effect of maleated PLA on the properties of rotomolded PLA-agave fiber biocomposites. *J Polym Environ* 27:61–73. <https://doi.org/10.1007/s10924-018-1308-2>
- Robledo-Ortiz JR, González-López ME, Martín del Campo AS et al (2021) Fiber-matrix interface improvement via glycidyl methacrylate compatibilization for rotomolded poly(lactic acid)/agave fiber biocomposites. *J Compos Mater* 55:201–212. <https://doi.org/10.1177/0021998320946821>
- León LDVE, Escocio VA, Visconte LLY et al (2020) Rotomolding and polyethylene composites with rotomolded lignocellulosic materials: a review. *J Reinf Plast Compos* 39:459–472. <https://doi.org/10.1177/0731684420916529>

21. Ortega Z, Romero F, Paz R et al (2021) Valorization of invasive plants from macaronesia as filler materials in the production of natural fiber composites by rotational molding. *Polymers (Basel)* 13:2220. <https://doi.org/10.3390/polym13132220>
22. Shatalov AA, Pereira H (2013) High-grade sulfur-free cellulose fibers by pre-hydrolysis and ethanol-alkali delignification of giant reed (*Arundo donax* L.) stems. *Ind Crops Prod* 43:623–630. <https://doi.org/10.1016/j.indcrop.2012.08.003>
23. Fiore V, Scalici T, Valenza A (2014) Characterization of a new natural fiber from *Arundo donax* L. as potential reinforcement of polymer composites. *Carbohydr Polym* 106:77–83. <https://doi.org/10.1016/j.carbpol.2014.02.016>
24. Suárez L, Castellano J, Romero F et al (2021) Environmental hazards of giant reed (*Arundo donax* L.) in the macaronesia region and its characterisation as a potential source for the production of natural fibre composites. *Polymers (Basel)*. <https://doi.org/10.3390/polym13132101>
25. Shatalov AA, Duarte LC, Carvalheiro F et al (2013) CROP-BIOREF: Integrated strategy for the upgrading of giant reed (*Arundo donax* L.) for materials and chemicals. *Proc 2nd Iber-oam Congr Biorefineries* 2013:641–648
26. Brusca S, Cosentino SL, Famoso F et al (2018) Second generation bioethanol production from *Arundo donax* biomass: an optimization method. *Energy Procedia*. Elsevier Ltd, Amsterdam
27. Shatalov AA, Pereira H (2012) Xylose production from giant reed (*Arundo donax* L.): modeling and optimization of dilute acid hydrolysis. *Carbohydr Polym* 87:210–217. <https://doi.org/10.1016/j.carbpol.2011.07.041>
28. Licursi D, Antonetti C, Mattonai M et al (2018) Multi-valorisation of giant reed (*Arundo Donax* L.) to give levulinic acid and valuable phenolic antioxidants. *Ind Crops Prod* 112:6–17. <https://doi.org/10.1016/j.indcrop.2017.11.007>
29. Antonetti C, Bonari E, Licursi D et al (2015) Hydrothermal conversion of giant reed to furfural and levulinic acid: optimization of the process under microwave irradiation and investigation of distinctive agronomic parameters. *Molecules* 20:21232–21353. <https://doi.org/10.3390/molecules201219760>
30. Calvo MV, Colombo B, Corno L et al (2018) Bioconversion of giant cane for integrated production of biohydrogen, carboxylic acids, and polyhydroxyalkanoates (PHAs) in a multistage biorefinery approach. *ACS Sustain Chem Eng* 6:15361–15373. <https://doi.org/10.1021/ACSSUSCHEMENG.8B03794>
31. Ventorino V, Robertiello A, Cimini D et al (2017) Bio-based succinate production from *Arundo donax* hydrolysate with the new natural succinic acid-producing strain *Basfia succiniciproducens* BPP7. *BioEnergy Res* 10:488–498. <https://doi.org/10.1007/s12155-017-9814-y>
32. Piperopoulos E, Khaskhoussi A, Fiore V, Calabrese L (2021) Surface modified *Arundo donax* natural fibers for oil spill recovery. *J Nat Fibers*. <https://doi.org/10.1080/15440478.2021.1961343>
33. Cano-Ruiz J, Ruiz Galea M, Amorós MC et al (2020) Assessing *Arundo donax* L in vitro-tolerance for phytoremediation purposes. *Chemosphere* 252:126576. <https://doi.org/10.1016/J.CHEMOSPHERE.2020.126576>
34. Raposo Oliveira Garcez L, Hofmann Gatti T, Carlos Gonzalez J et al (2022) Characterization of fibers from culms and leaves of *Arundo donax* L (Poaceae) for handmade paper production. *J Nat Fibers*. <https://doi.org/10.1080/15440478.2022.2076005>
35. Gulihonenahali Rajkumar A, Hemath M, Kurki Nagaraja B et al (2021) An artificial neural network prediction on physical, mechanical, and thermal characteristics of giant reed fiber reinforced polyethylene terephthalate composite. *J Ind Text*. <https://doi.org/10.1177/15280837211064804>
36. Dahmardeh Ghalehno M, Madhoushi M, Tabarsa T, Nazerian M (2010) The manufacture of particleboards using mixture of reed (surface layer) and commercial species (middle layer). *Eur J Wood Wood Prod* 693(69):341–344. <https://doi.org/10.1007/S00107-010-0437-7>
37. Ferrandez-García MT, Ferrandez-García A, Garcia-Ortuño T et al (2020) Assessment of the physical, mechanical and acoustic properties of *Arundo donax* L biomass in low pressure and temperature particleboards. *Polymers* 12:1361. <https://doi.org/10.3390/POLYM12061361>
38. Fiore V, Botta L, Scaffaro R et al (2014) PLA based biocomposites reinforced with *Arundo donax* fillers. *Compos Sci Technol* 105:110–117. <https://doi.org/10.1016/j.compscitech.2014.10.005>
39. Monsalve Alarcón J, Sánchez Cruz M, Baquero Bastos D (2018) Evaluation of the physical and mechanical properties of caña brava (*Arundo donax*) reinforced panels. *INGE CUC* 14:66–74. <https://doi.org/10.17981/ingecuc.14.1.2018.06>
40. Fiore V, Scalici T, Vitale G, Valenza A (2014) Static and dynamic mechanical properties of *Arundo donax* fillers-epoxy composites. *Mater Des* 57:456–464. <https://doi.org/10.1016/j.matdes.2014.01.025>
41. Scalici T, Fiore V, Valenza A (2016) Effect of plasma treatment on the properties of *Arundo donax* L. leaf fibres and its bio-based epoxy composites: a preliminary study. *Compos Part B Eng* 94:167–175. <https://doi.org/10.1016/j.compositesb.2016.03.053>
42. Comité Técnico CTN 53 (2008) UNE-CEN/TR 15351 IN: plásticos. Guía terminológica en el campo de los plásticos y polímeros degradables y biodegradables
43. Shah AA, Hasan F, Hameed A, Ahmed S (2008) Biological degradation of plastics: a comprehensive review. *Biotechnol Adv* 26:246–265. <https://doi.org/10.1016/j.biotechadv.2007.12.005>
44. Husárová L, Pekařová S, Stloukal P et al (2014) Identification of important abiotic and biotic factors in the biodegradation of poly(l-lactic acid). *Int J Biol Macromol* 71:155–162. <https://doi.org/10.1016/J.IJBIOMAC.2014.04.050>
45. Agarwal M, Koelling KW, Chalmers JJ (1998) Characterization of the degradation of polylactic acid polymer in a solid substrate environment. *Biotechnol Prog* 14:517–526. <https://doi.org/10.1021/BP980015P>
46. Ruggero F, Belardi S, Carretti E et al (2022) Rigid and film bioplastics degradation under suboptimal composting conditions: a kinetic study. *Waste Manag Res* 40:1311–1321. <https://doi.org/10.1177/0734242X211063731>
47. Boonmee C, Kositanont C, Leejarkpai T (2022) Degradation behavior of biodegradable plastics in thermophilic landfill soil and wastewater sludge conditions. *Environ Res Eng Manag* 78:57–69. <https://doi.org/10.5755/J01.EREM.78.1.29502>
48. Gorrasi G, Pantani R (2013) Effect of PLA grades and morphologies on hydrolytic degradation at composting temperature: assessment of structural modification and kinetic parameters. *Polym Degrad Stab* 98:1006–1014. <https://doi.org/10.1016/J.POLYMDEGRADSTAB.2013.02.005>
49. Cucina M, De Nisi P, Trombino L et al (2021) Degradation of bioplastics in organic waste by mesophilic anaerobic digestion, composting and soil incubation. *Waste Manag* 134:67–77. <https://doi.org/10.1016/J.WASMAN.2021.08.016>
50. Oliveira MAS, Pickering KL, Sunny T, Lin RJT (2021) Treatment of hemp fibres for use in rotational moulding. *J Polym Res* 28:3. <https://doi.org/10.1007/s10965-021-02414-3>
51. Bayerl T, Geith M, Somashekar AA, Bhattacharyya D (2014) Influence of fibre architecture on the biodegradability of FLAX/PLA composites. *Int Biodeterior Biodegrad* 96:18–25. <https://doi.org/10.1016/j.ibiod.2014.08.005>
52. Moliner C, Finocchio E, Arato E et al (2020) Influence of the degradation medium on water uptake, morphology, and chemical structure of poly(lactic acid)-sisal bio-composites. *Materials (Basel)* 13:3974. <https://doi.org/10.3390/ma13183974>

53. Dong Y, Ghataura A, Takagi H et al (2014) Polylactic acid (PLA) biocomposites reinforced with coir fibres: evaluation of mechanical performance and multifunctional properties. *Compos Part A Appl Sci Manuf* 63:76–84. <https://doi.org/10.1016/j.compositesa.2014.04.003>
54. Hanana FE, Rodrigue D (2021) Effect of particle size, fiber content, and surface treatment on the mechanical properties of maple-reinforced LLDPE produced by rotational molding. *Polym Polym Compos* 29:343–353. <https://doi.org/10.1177/0967391120916602>
55. Cisneros-López EO, González-López ME, Pérez-Fonseca AA et al (2017) Effect of fiber content and surface treatment on the mechanical properties of natural fiber composites produced by rotomolding. *Compos Interfaces* 24:35–53. <https://doi.org/10.1080/09276440.2016.1184556>
56. Monzón MD, Ortega Z, Benítez AN et al (2012) Developments towards a more sustainable rotational moulding process. *ECCM 2012 Compos Venice Proc 15th Euro Conf Compos Mater* 2012:1–8
57. Abhilash SS, Singaravelu DL (2020) Effect of fiber content on mechanical and morphological properties of bamboo fiber-reinforced linear low-density polyethylene processed by rotational molding. *Trans Indian Inst Met* 73:1549–1554. <https://doi.org/10.1007/s12666-020-01922-y>
58. Höfler G, Lin RJT, Jayaraman K (2018) Rotational moulding and mechanical characterisation of halloysite reinforced polyethylenes. *J Polym Res*. <https://doi.org/10.1007/s10965-018-1525-3>
59. Huda MS, Drzal LT, Mohanty AK, Misra M (2007) The effect of silane treated- and untreated-talc on the mechanical and physico-mechanical properties of poly(lactic acid)/newspaper fibers/talc hybrid composites. *Compos Part B Eng* 38:367–379. <https://doi.org/10.1016/J.COMPOSITESB.2006.06.010>
60. Fritz M, Lauschke T, Schlebrowski T et al (2022) Photoaging phenomena of biodegradable polybutylene succinate and conventional low density polyethylene by artificial weathering – a comparative surface study. *Appl Surf Sci* 590:153058. <https://doi.org/10.1016/J.APSUSC.2022.153058>
61. Huang C, Liao Y, Zou Z et al (2022) Novel strategy to interpret the degradation behaviors and mechanisms of bio- and non-degradable plastics. *J Clean Prod* 355:131757. <https://doi.org/10.1016/J.JCLEPRO.2022.131757>
62. Arrieta MP, López J, Rayón E, Jiménez A (2014) Disintegrability under composting conditions of plasticized PLA–PHB blends. *Polym Degrad Stab* 108:307–318. <https://doi.org/10.1016/J.POLYMDEGRADSTAB.2014.01.034>

Publisher's Note Springer Nature remains neutral with regard to jurisdictional claims in published maps and institutional affiliations.